A Commutation Torque Ripple Reduction for Brushless DC Motor Drives

Chang-hee Won*, Joong-Ho Song and Ick Choy*****

Abstract - This paper presents a comprehensive study on reducing commutation torque ripples generated in brushless DC motor drives with only a single dc-link current sensor provided. In such drives, commutation torque ripple suppression techniques that are practically effective in low speed as well as high speed regions are scarcely found. The commutation compensation technique proposed here is based on a strategy that the current slopes of the incoming and the outgoing phases during the commutation interval can be equalized by a proper duty-ratio control. Being directly linked with deadbeat current control scheme, the proposed control method accomplishes suppression of the spikes and dips superimposed on the current and torque responses during the commutation intervals of the inverter. Effectiveness of the proposed control method is verified through simulations and experiments.

Keywords: commutation torque ripple, brushless DC motor, deadbeat current controller, dc-link current sensor

1. Introduction

Brushless DC motors with trapezoidal back-EMF have been widely used due to their high power density and easy control method. Moreover, basic trapezoidal brushless DC motors make it possible to use a single DC-link current sensor to regulate the phase current flowing through two motor phases. When 120° rectangular stator current control is performed based on a single current sensor as shown in Fig.1, commutation torque ripples usually occur due to the loss of exact phase current control during the phase current commutation intervals. Fig.2, as a typical example, shows the commutation torque ripple in trapezoidal brushless DC motors, including torque spikes in the low speed range and torque dips in the high speed range. A theoretical analysis related to these commutation torque ripples is found in literature [1, 2]. As for brushless DC motor drives with three phase current sensors, many researches regarding commutation torque ripple have been carried out [1-4].

Methods for reducing the commutation torque ripple in brushless DC motors with a single current sensor have been reported in several literatures. A phase voltage control adjusts duty ratio applied during commutation intervals to reduce the torque ripple [4]. An overlap switching method by which the turn-off timing instant of the outgoing switch is delayed is presented [5]. A current control with a chopping action activated only during commutation intervals reduces the current peak appeared in the uncommutated phase [6]. However, these conventional methods show limited effectiveness in practical applications due to motor parameter sensitivity and unsatisfactory performance over a wide speed range.

This paper presents a comprehensive analysis of the commutation torque ripple suppression method in brushless DC motor drives with only a single current sensor. A deadbeat current controller is employed to enhance the current control performance. The proposed control scheme makes the commutation current slopes of the incoming and outgoing phases balanced during the commutation interval of the phase currents. This new torque ripple suppression technique provides attractive performance over the wide speed range.

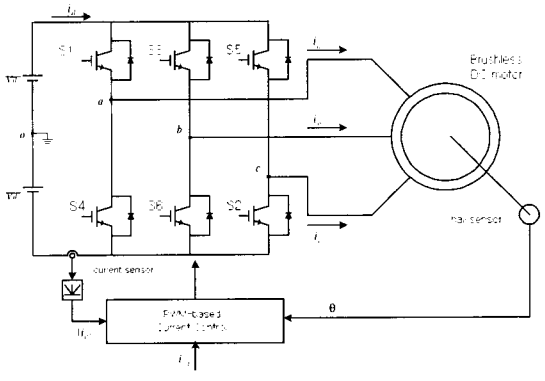

(a)

* Mechatronics Center, Samsung Electronics Co. Korea.
** Department of Electrical Engineering, Seoul National University of Technology, Korea.
*** Korea Institute of Science and Technology, Korea.
Received April 29, 2002 ; Accepted Augest 9, 2002

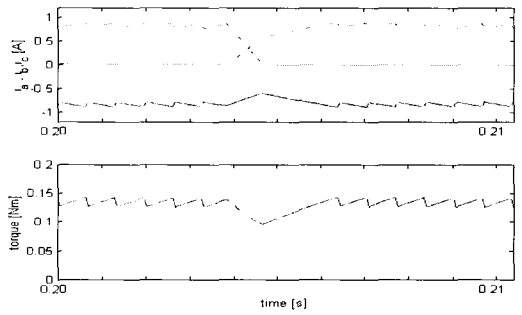

(b)

Fig. 2 Typical forms of commutation torque ripple; (a) in low speed, (b) in high speed

2. Current Control

2.1 Normal mode

Fig. 3 shows phase currents, dc-link current, and equivalent circuits when inverter switches S2 and S3 operate in PWM mode. According to the switching conditions of the inverter switches, the voltage equations related to the switch-on and switch-off intervals in the normal operation mode can be described as the following equations (1) and (2), respectively,

$$v_{bc} = V_d = 2R \cdot i_d + 2L\frac{di_d}{dt} + e_{bc} \tag{1}$$

$$v_{bc} = -V_d = -2R \cdot i_d - 2L\frac{di_d}{dt} + e_{bc} \ . \tag{2}$$

Combining equations (1) and (2) by introducing the switching function S, the resultant voltage equation can be rearranged as

$$S \cdot V_d = 2R \cdot |i_d| + 2L\left|\frac{di_d}{dt}\right| + 2E \ , \tag{3}$$

where S denotes 1 for switch-on and -1 for switch-off and E means the magnitude of the back-EMF.

Considering the signs of the switching function S and the dc-link current, the following equation is formulated for the deadbeat current controller based on the dc-link current measured. It is noted in this equation that the information required about back-EMF is not the overall waveform, but the magnitude value E in the flat top part of the back-EMF waveform. The output signal of the deadbeat current controller is expressed as

$$V_m^*(k) = K_1 \cdot |i_d(k-1)| + K_2 \cdot \left(i_d^*(k-1) - |i_d(k-1)|\right) + 2E(k-1) \ , \tag{4}$$

where K_1, K_2, and T_s denote $2R$, $2L/T_s$, and sampling interval, respectively.

2.2 Commutation mode

When the deadbeat controller equation used in the normal mode is directly applied to the commutation mode, the

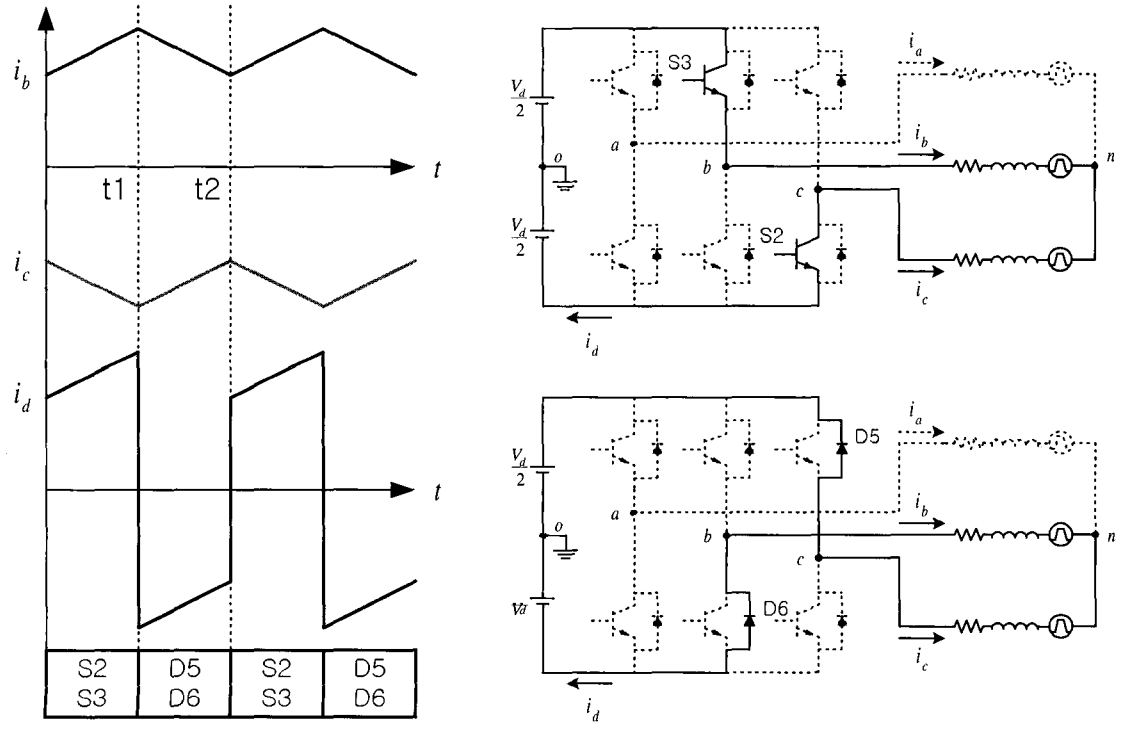

Fig. 3 Normal mode operation

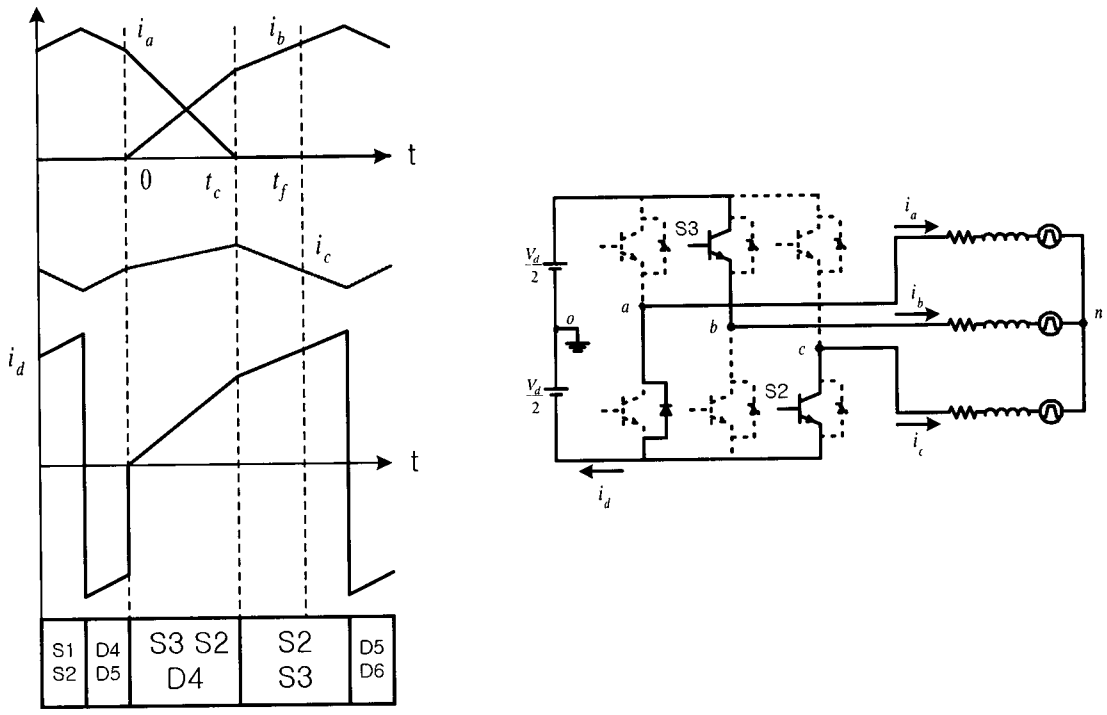

(a)

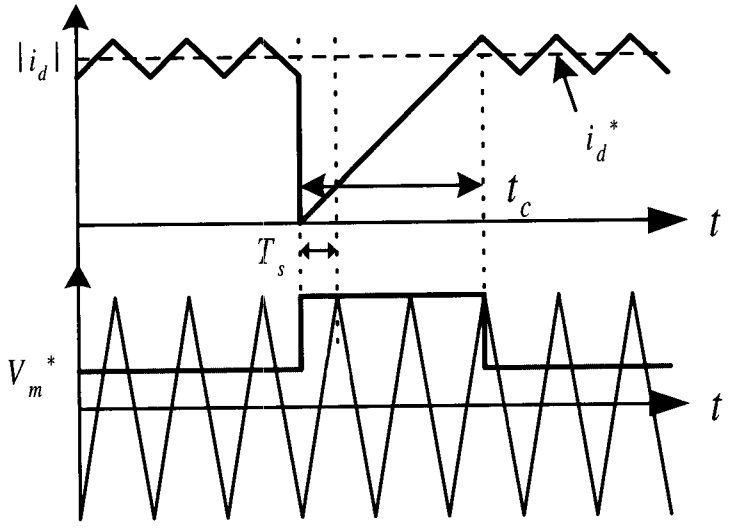

(b)

Fig. 4 Commutation mode operation; (a) equivalent circuit and flowing currents, (b) saturation of deadbeat current controller

resulting waveforms are shown in Fig. 4. This figure shows that control of dc-link current cannot be accomplished exactly during commutation interval. Since the dc-link current cannot be tightly controlled close to the current reference value within a sampling interval T_s, the corresponding terminal voltage reference value V_m^* reaches a certain saturation level, $V_{m,sat}$. As a result, such a saturation phenomenon of the current controller provokes commutation torque ripples during commutation intervals. Current spikes and dips imposed on the un-commutated phase current waveform are known to reflect the corresponding commutation torque ripple on the generated torque. This problem can be suppressed by using a commutation reduction technique proposed in the following section.

3. Torque Ripple reduction

It is seen in the preceding section that a basic deadbeat current controller can provide no plausible reduction in commutation torque ripple because of the controller satu-

ration during commutation period. In order to resolve the problem, a control technique that can compensate for the saturated output signal of the controller and equalize the slopes of the two commutated phase currents is described in this section.

3.1 Low speed region ($V_d > 4E$)

Fig. 5 shows the switching sequence and the respective phase current waveforms during commutation interval in the low speed region. Dotted lines describe the phase current waveforms and switching patterns S1′, S2′, S3′ when deadbeat current controller is saturated as explained in the preceding section. It is realized that a method to slow down the rising time of the incoming phase current i_b can be a desirable technique to equalize the mismatched commutation times of the two commutated phase currents. Solid lines show the waveforms corresponding to the case in which the PWM patterns S1, S2, and S3, which take duty ratio D_{low} designed especially for the commutation interval, are applied to the inverter. The inverter output voltage driven by the PWM patterns S1, S2, S3 is modulated at duty ratio D_{low} to equalize the slopes of the incoming phase current i_b and the outgoing phase current i_a. Referring to Fig. 5, phase voltage equations during commutation interval can be described as equations (5)-(7) and the neutral voltage is given by equation (8).

$$-\frac{V_d}{2} = R \cdot i_a + L\frac{di_a}{dt} + e_a + V_{no} \tag{5}$$

$$S \cdot \frac{V_d}{2} = R \cdot i_b + L\frac{di_b}{dt} + e_b + V_{no} \tag{6}$$

$$-S \cdot \frac{V_d}{2} = R \cdot i_c + L\frac{di_c}{dt} + e_c + V_{no} \tag{7}$$

$$V_{no} = -\frac{V_d}{6} - \frac{e_a + e_b + e_c}{3} \tag{8}$$

In this commutation interval, it is assumed that the motor winding resistance is neglected, and e_a and e_b maintain the value of E and e_c holds at $-E$. The slope of the A-phase current i_a can be described as

$$\frac{di_a}{dt} = \frac{1}{L}\left(-\frac{V_d}{2} - e_a - v_{no}\right) = -\frac{V_d + 2E}{3L} . \tag{9}$$

The slope of the B-phase current is calculated according to the switching function as follows.

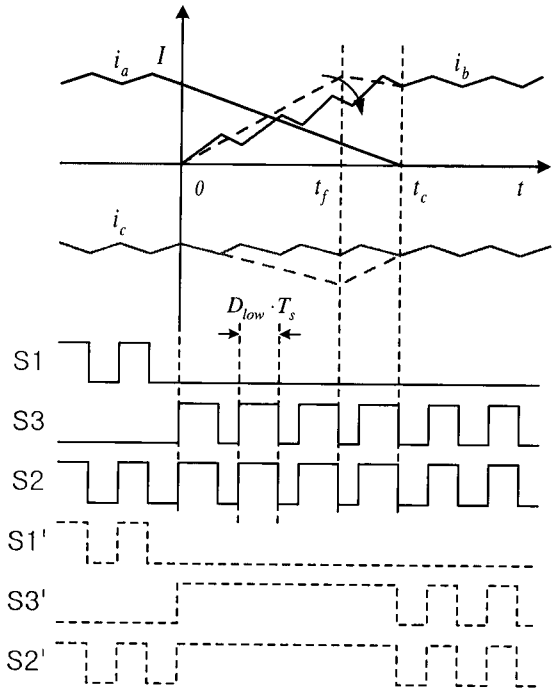

Fig. 5 Switching patterns and commutation in low speed

$$\begin{cases} \dfrac{di_b}{dt} = \dfrac{2(V_d - E)}{3L}, & \text{at } S = 1 \\ \dfrac{di_b}{dt} = -\dfrac{V_d + E}{3L}, & \text{at } S = -1 \end{cases} \tag{10}$$

The slope equation corresponding to the switching state, in which S maintains 1 during $D_{low}T_s$ and -1 during $(1-D_{low})T_s$, can be arranged using a state-space averaging technique.

$$\frac{di_b}{dt} = \frac{V_d(3D_{low} - 1) - 2E}{3L} \tag{11}$$

It is desired that the slope of the incoming phase current of equation (9) is equal to that of the outgoing phase current of equation (11) during commutation interval. From equations (9) and (11), therefore, the resultant duty ratio D_{low} is obtained as

$$D_{low} = \frac{2}{3} + \frac{4E}{3V_d} = \frac{1}{3}\left(2 + \frac{4E}{V_d}\right). \tag{12}$$

3.2 High speed region ($V_d < 4E$)

Similarly, it is noted in high speed region as shown in Fig. 6 that a method to slow down the falling time of the outgoing phase current i_a becomes a desirable strategy to equalize the mismatched commutation times of the two

commutated phase currents. Referring to Fig. 6, the following equations can be derived to accomplish the torque ripple reduction in the high speed region.

$$S \cdot \frac{V_d}{2} = R \cdot i_a + L\frac{di_a}{dt} + e_a + V_{no} \tag{13}$$

$$\frac{V_d}{2} = R \cdot i_b + L\frac{di_b}{dt} + e_b + V_{no} \tag{14}$$

$$-\frac{V_d}{2} = R \cdot i_c + L\frac{di_c}{dt} + e_c + V_{no} \tag{15}$$

$$V_{no} = S \cdot \frac{V_d}{6} - \frac{e_a + e_b + e_c}{3} \tag{16}$$

When the switching function S is 1, the undergoing current slopes can be described as

$$\frac{di_a}{dt} = \frac{V_d - 2E}{3L} \tag{17}$$

$$\frac{di_b}{dt} = \frac{V_d - 2E}{3L}. \tag{18}$$

When S becomes –1, the equations are written as

$$\frac{di_a}{dt} = -\frac{V_d + 2E}{3L} \tag{19}$$

$$\frac{di_b}{dt} = \frac{2(V_d - E)}{3L}. \tag{20}$$

From equations (17) – (20), the resulting equations can be obtained using a state-space averaging technique.

$$\frac{di_a}{dt} = -\frac{V_d(2D_{high} - 1) - 2E}{3L} \tag{21}$$

$$\frac{di_b}{dt} = \frac{V_d(2 - D_{high}) - 2E}{3L} \tag{22}$$

From equations (21) and (22), finally, the duty ratio D_{high} is arranged as

$$D_{high} = \frac{4E}{V_d} - 1. \tag{23}$$

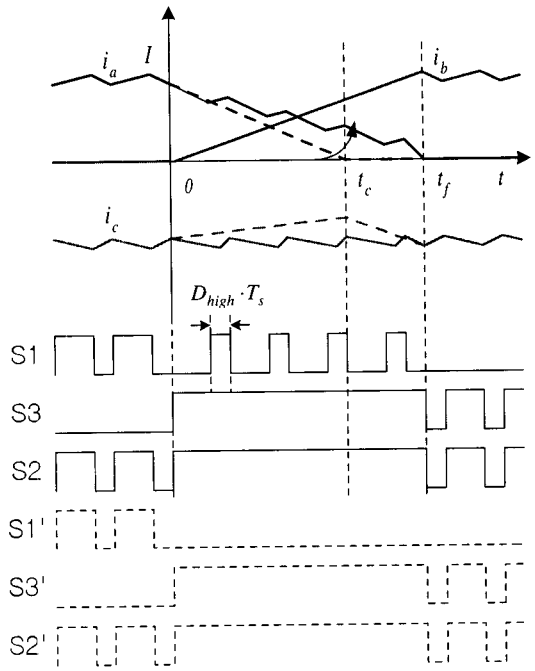

Fig. 6 Switching patterns and commutation in high speed

Looking into equations (12) and (23), the duty ratio applied to the inverter during commutation interval is found to have no relation with the inductance of the motor. The relation between the duty ratio and a variable $4E/V_d$ is plotted by equations (12) and (23) as shown in Fig. 7.

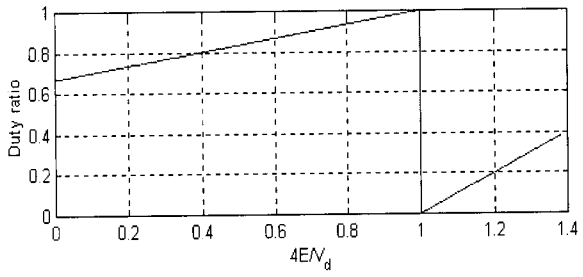

Fig. 7 Duty ratio for commutation compensation

3.3 Combination with deadbeat controller

As shown in Fig. 8, the duty ratios derived in section 3.2 can be combined with deadbeat current controller. Such a control scheme allows the deadbeat controller to be in action as well as to compensate the saturated output signal even during the commutation interval.

The saturated value $V_{m,sat}$ of the basic deadbeat current controller is released by a saturation-compensating signal v_{comp}. Using a graphical representation shown in Fig. 9(a), the saturation-compensating signal v_{comp} can be computed in the function of the duty ratios D_{low} and D_{high} as equations (24) and (25) in the low and high speed ranges, respectively.

$$v_{comp} = 2V_d(1 - D_{low}) \quad (24)$$

$$v_{comp} = 2V_d \cdot D_{high} \quad (25)$$

Fig. 9(b), which describes equations (24) and (25) and Fig. 7, shows a function between the counter EMF magnitude and the compensating signal v_{comp}. In the low speed range, v_{comp} decreases gradually as the motor speed increases, whereas v_{comp} increases rapidly in proportion to the motor speed in the high-speed region. It is also seen that v_{comp} becomes zero at the motor speed corresponding to $V=4E$.

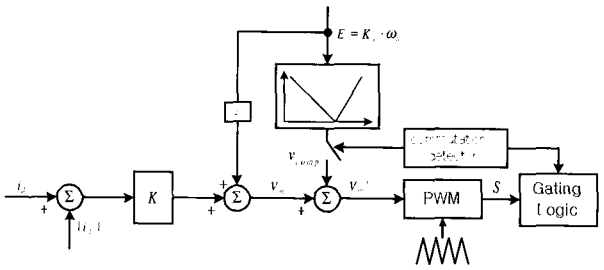

Fig. 8 Deadbeat current controller with commutation compensation

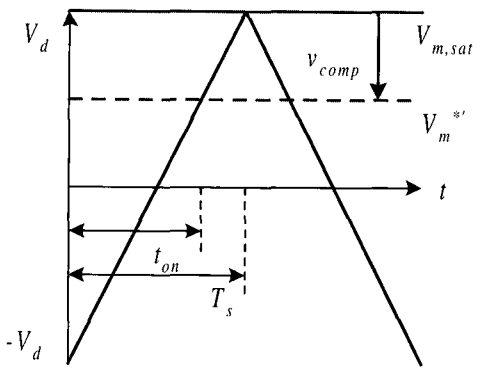

(a)

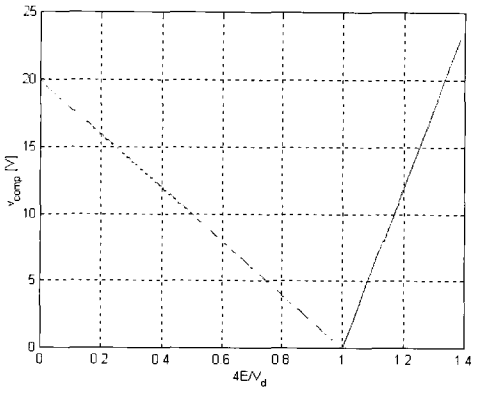

(b)

Fig. 9 Commutation compensation level; (a) compensation level calculation, (b) commutation compensation level and counter EMF

4. Simulation and ExperimentATION

To verify the feasibility of the proposed algorithm, simulations and experiments are carried out. A brushless DC motor with a nameplate data of 4 poles, 40V, 45W, and 1500 rpm is dealt with in this paper. To implement the proposed algorithm, the TMS320F243 DSP is employed in the control board set-up. PI speed control, deadbeat current control, and commutation compensation loops operate every 50μ s sampling time. Figs. 10 and 11 show the simulation results of the phase currents, DC-link current, and torque ripple obtained in the low speed range of 200rpm and in the high speed range of 1200rpm, respectively. In Figs. 10 and 11, the left-hand side figures show the responses in the case of a control scheme with no compensation loop, whereas the right-hand side figures show the responses with the compensation loop. These figures show that the proposed compensation technique is very effective on the commutation torque ripple suppression over the wide motor speed range. Note that since a torque meter is unavailable in the experimental set-up, phase current waveforms that sufficiently reflect the commutation torque ripples are monitored instead of the actual torque ripples. When the motor rotates at low speed, experimental results related to the C-phase current spike are shown in Fig. 12. Fig. 12(a) shows the phase current spike generated during the commutation time interval when the deadbeat controller without commutation compensation is used for current regulation. In Fig. 12(b), where the proposed compensation algorithm is in use, the phase current spike hardly appears. Fig. 13 shows the C-phase current waveform when the motor rotates at high speed. The phase current dip exists when the compensation loop is not used; the dip, on the contrary, is eliminated when the compensation loop is employed. From this commutation current ripple suppression, therefore, it is noted that the resulting commutation torque ripples are effectively suppressed over the entire speed range with the help of the proposed compensation algorithm. Figs. 14 and 15 show the switching signals of the inverter switches and the commutation processing responses of the respective phase currents in the low speed and the high speed ranges, respectively. These figures show that the proposed algorithm makes it possible to effectively equalize the mismatched commutation times of the two commutated phase currents.

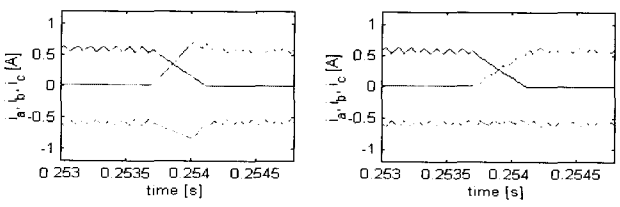

(a)

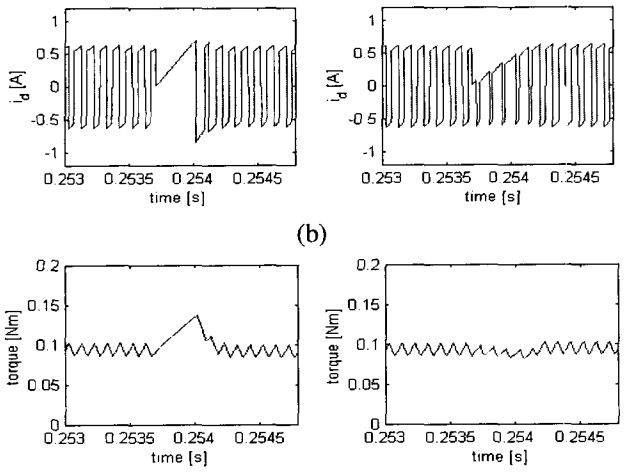

Fig. 10 Simulation results in the low speed; (a) phase currents, (b) DC-link current, (c) commutation torque ripple

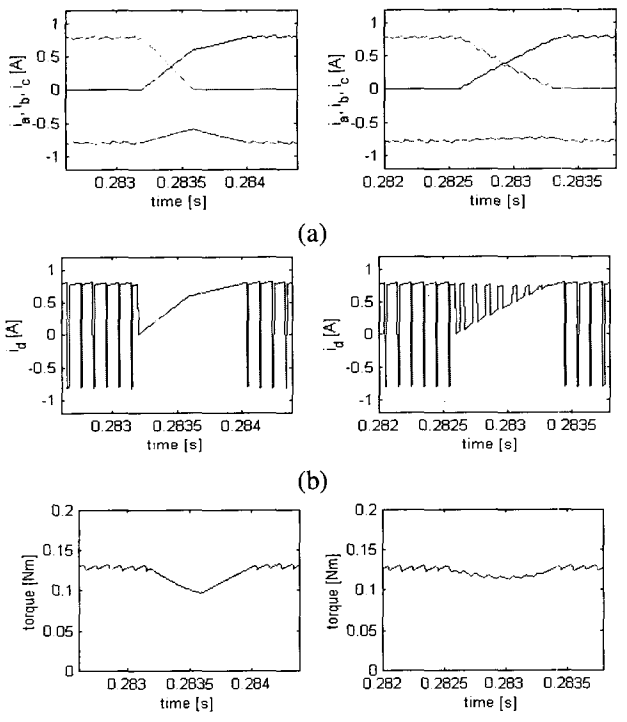

Fig. 11 Simulation results in the high speed; (a) phase currents, (b) DC-link current, (c) commutation torque ripple

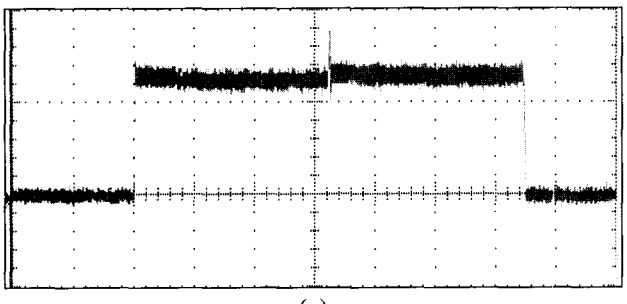

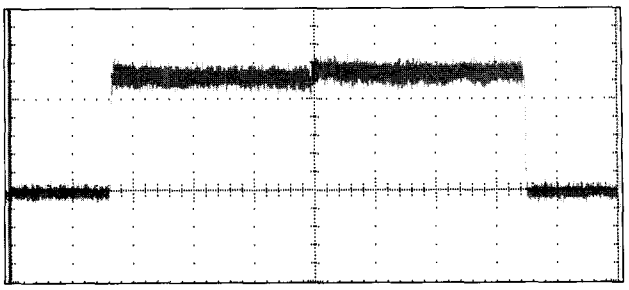

Fig. 12 Experimental results in the low speed (0.5 A/div, 10ms/div): (a) without compensation, (b) with compensation

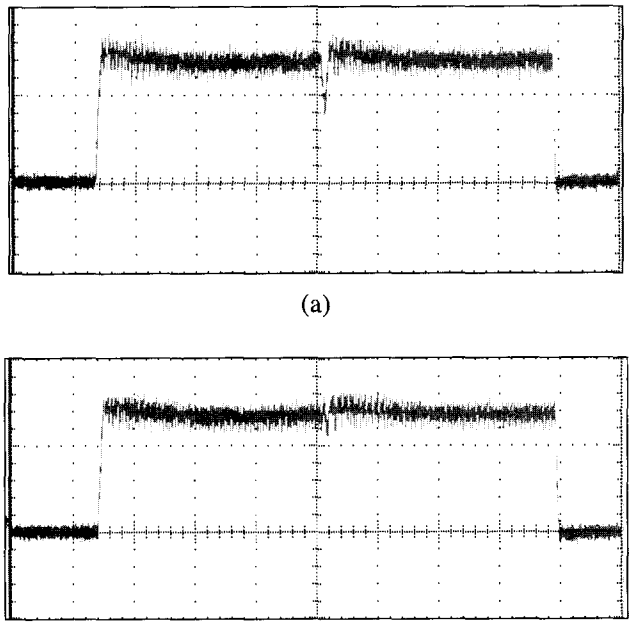

Fig. 13 Experimental results in the high speed (0.5 A/div, 4ms/div): (a) without compensation, (b) with compensation

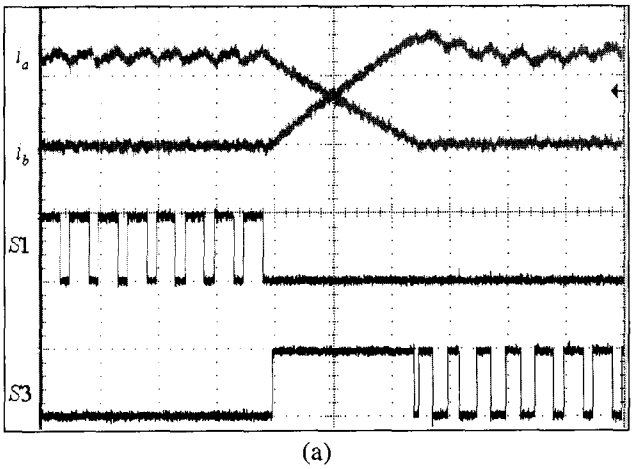

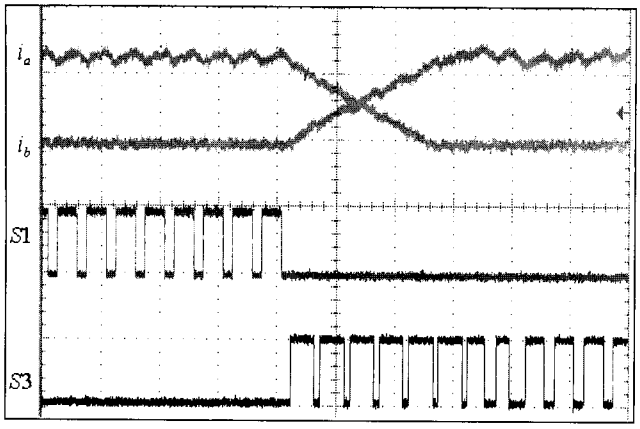

(b)

Fig. 14 Commutation currents and switching pattern in the low speed (0.5 A/div, 100μs/div): (a) without compensation, (b) with compensation

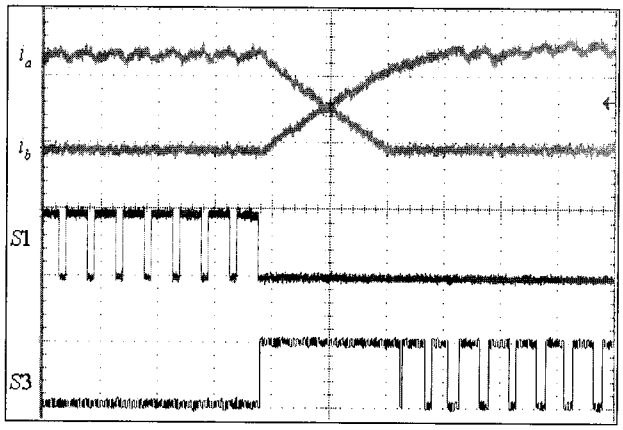

(a)

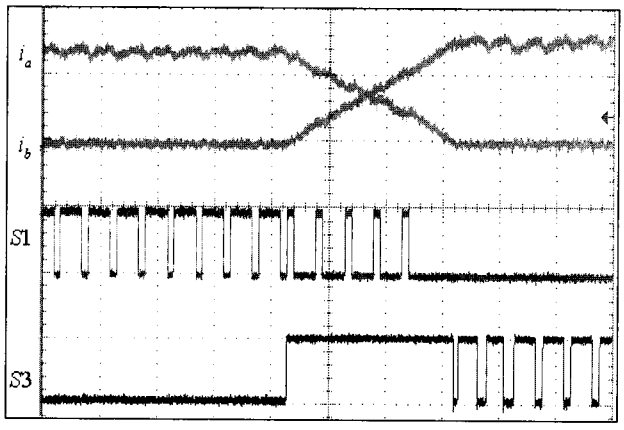

(b)

Fig. 15 Commutation currents and switching pattern in the high speed (0.5 A/div, 100μs/div): (a) without compensation, (b) with compensation

5. Conclusion

In this paper, a commutation torque ripple reduction method has been proposed for brushless DC motor drives using a single DC current sensor. In such drives, the DC-link current sensor cannot give any information corresponding to the motor currents during the phase current commutation intervals. Using the commutated phase current waveforms synthesized from the measured DC current, a duty ratio control strategy has been devised to equalize the two mismatched commutation time intervals. By being directly linked with the deadbeat current control scheme, the proposed control method accomplishes successful suppression of the spikes and dips superimposed on the current and torque responses during the commutation intervals. This scheme shows attractive effectiveness in the low and the high speed regions through simulations and experiments.

References

[1] T. M. Jahns and W. L. Soong, "Pulsating torque minimization techniques for permanent magnet AC motor drives - a Review," *IEEE Trans. on Industrial Electronics*, vol. 43, no. 2, pp. 321-330, 1996.

[2] R. Carlson, M. Lajoie-Mazenc, and J. C. S. Fagundes, "Analysis of torque ripple due to phase commutation in brushless DC machines," *IEEE Trans. on Industry Applications*, vol. 28, no. 3, pp. 632-638, 1992.

[3] K.-W. Lee, J.-B. Park, H.-G. Yeo, J.-Y. Yoo, and H.-M. Jo, "Current control algorithm to reduce torque ripple in brushless dc motors," *International Conference on Power Electronics*, pp. 380-385, 1998.

[4] J. Cros, J. M. Vinassa, S. Clenet, S. Astier, and M. Lajoie-Mazenc, "A novel current control strategy in trapezoidal EMF actuators to minimize torque ripples due to phases commutations," *European Power Electronics Conference*, pp. 266-271, 1993.

[5] Y. Murai, Y. Kawase, K. Ohashi, K. Nagatake, and K. Okuyama," Torque ripple improvement for brushless dc miniature motors," *IEEE Trans. on Industry Applications*, vol. 25, no. 3, pp. 441-450, 1989.

[6] L. Schlting and H.–C. Skudenly, "A control method for permanent magnet synchronous motors with trapezoidal electromotive force," *European Power Electronics Conference*, pp. 117-122, 1991.

Chang-hee Won

He received the B.S. degree from Seoul National University of Technology in 2000 and the M.S. degree from Korea University, Korea, in 2002. From 2000 to 2002, he worked as a student researcher in the Intelligent System Control Research Center, Korea Institute of Science and Technology. Since 2002, he has been with the Mechatronics Center, Samsung Electronics Co. His main research interests include microprocessor applications and high-performance drives.

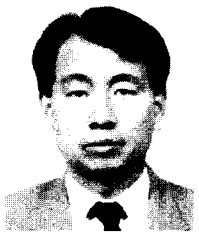

Joong-Ho Song

He received the B.S. and M.S. degrees from Seoul National University, respectively, in 1980 and 1986, and the Ph.D. degree from Korea Advanced Institute of Science and Technology, Korea, in 1993. He worked as an engineer for E-hwa Electrical Co., Korea, from 1982 to 1985. From 1985 to 2002, he was with the Intelligent System Control Research Center, Korea Institute of Science and Technology. Since 2002, he has been with the Department of Electrical Engineering, Seoul National University of Technology. He was a visiting scholar in University of Wisconsin-Madison, in 1995-1996. His primary research interests are switching converters, electric machine drives, and servo control technologies.

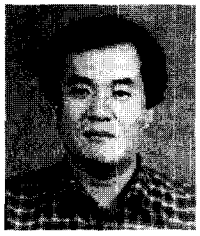

Ick Choy

He received the B.S., M.S., and Ph.D. degrees from Seoul National University, Korea, in 1979, 1981, and 1990, respectively. Since 1981, he has been with the Intelligent System Control Research Center, Korea Institute of Science and Technology. His main research interests include microprocessor applications, high-performance drives, and emerging technologies.